

壳聚糖作用下一步法合成具有高电活性的 AgCl@ 聚苯胺核壳结构

冯晓苗 叶青青 侯文华* 朱俊杰*
(南京大学化学化工学院, 南京 210093)

摘要: 在壳聚糖的作用下, 采用简单的一步法合成了具有星状结构的氯化银/聚苯胺核壳型复合材料。当壳聚糖的浓度为 1% 时, 所制备的氯化银/聚苯胺复合材料具有高度的分散性, 壳层厚度为 30~80 nm, 核的直径在 25~60 nm 范围内。通过透射电镜、红外光谱和 X-射线衍射对样品的形态和组成进行了表征。循环伏安实验结果表明这种复合材料在中性条件下具有很好的电化学活性。

关键词: 氯化银; 聚苯胺; 核壳; 电化学活性

中图分类号: O614.122

文献标识码: A

文章编号: 1001-4861(2007)09-1572-05

One Step Synthesis of AgCl@Polyaniline Core-shell Nanostructure with Enhanced Electrochemical Activity in the Presence of Chitosan

FENG Xiao-Miao YE Qing-Qing HOU Wen-Hua* ZHU Jun-Jie*
(School of Chemistry and Chemical Engineering, Nanjing University, Nanjing 210093)

Abstract: Silver chloride@polyaniline (PANI) core-shell composites with a star-like structure were synthesized through a facile one-step process in the presence of chitosan. When the chitosan concentration was 1%, highly dispersed AgCl@PANI core-shell nanostructure with a shell thickness of 30~80 nm and a core diameter of 25~60 nm could be obtained. The morphology and composition were characterized by transmission electron microscopy (TEM), Fourier transform infrared (FTIR) and X-ray diffraction (XRD). Cyclic voltammetric experiments indicated that this kind of material showed excellent electrochemical activity in neutral pH environment.

Key words: silver chloride; polyaniline; core-shell; electrochemical activity

0 Introduction

The synthesis of materials with controlled size and morphology is an important factor for defining properties such as the electronic band gap, conductivity and light emission efficiency^[1]. Three-dimensional (3D) nanomaterials with core-shell structure, located in the transition region between atoms and bulk solids, are interesting in the fields of catalysis, biosensor, and light-emitting devices because of their large BET

surface area, particle size and quantum effect^[2].

Conducting polymer/inorganic nanocomposites with different combinations of the two components have attracted more and more attention, since they have interesting physical properties and many potential applications^[3]. As one of the most important conducting polymers, polyaniline (PANI) has been intensively studied in recent years. This is mainly because it has many advantages such as easy synthesis and good environmental stability as well as electronic, biological,

收稿日期: 2007-05-08。收修改稿日期: 2007-07-06。

国家自然科学基金资助项目(No.20635020, 90606016); 国家基础研究项目(No.2003CB615804); 南京大学分析测试基金。

*通讯联系人。E-mail: jjzhu@nju.edu.cn; whou@nju.edu.cn; Tel&Fax: 025-83594976

第一作者: 冯晓苗, 女, 29岁, 博士研究生; 研究方向: 复合材料与电化学。

and optical properties^[4-7]. The fabrication of nanocomposites containing PANI and a large variety of inorganic nanoparticles with core-shell structure have been reported^[8-10].

However, PANI is redox-active only at acidic conditions, generally at $\text{pH} < 4$ ^[11], this greatly restricts its applications in bioelectrochemistry, which normally needs a neutral pH environment. Many effective efforts have been directed towards enhancing the redox-active of PANI either by introducing acidic groups into the PANI chains or doping PANI with negatively charged polyelectrolytes^[12,13]. Some of these materials have been successfully used to immobilize enzymes^[14].

We synthesized AgCl@PANI nanocomposites with core-shell structure in the presence of chitosan in this work. Herein, chitosan as an anchor agent promoted a strong interaction between AgCl particles and aniline monomer, leading to the formation of AgCl@PANI core-shell structure. The morphology and composition were characterized by transmission electron microscopy (TEM), Fourier transform infrared (FTIR) and X-ray diffraction (XRD). Cyclic voltammetric experiments indicated that this kind of material showed excellent electrochemical activity.

1 Experimental

1.1 Materials

Aniline, silver nitrate (AgNO_3), hydrochloric acid (HCl) and ammonium persulfate ($(\text{NH}_4)_2\text{S}_2\text{O}_8$, APS) were purchased from Shanghai Chemical Reagent Co. The deacetylation degree of chitosan (Nantong Shuanglin Biological Product Inc.) was about 95%. Aniline was distilled under reduced pressure and other reagents were used as received without further treatment.

1.2 Synthesis of AgCl@PANI core-shell composites

AgNO_3 (0.01 g) and aniline (0.05 mmol) were added to 20 mL of chitosan acetic acid solution. 5 mL of $1 \text{ mol} \cdot \text{L}^{-1}$ HCl aqueous solution of APS as oxidant was added dropwise into the above mixture under stirring at room temperature. The molar ratio of aniline to APS ($n_{\text{An}}:n_{\text{APS}}$) was 1:1. The reaction was allowed to proceed for 24 h to obtain the composites. After that, the pre-

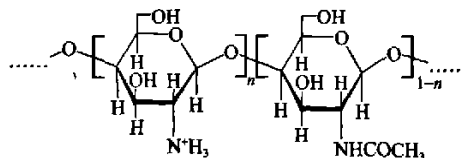
cipitate was centrifuged and washed several times with distilled water and ethanol. The final product was dried in vacuum at $60 \text{ }^\circ\text{C}$ for 24 h.

1.3 Characterization

The core-shell structure of AgCl@PANI was verified by transmission electron microscopy (TEM, JEOL JEM-200CX). Powder X-ray diffraction patterns (XRD) were taken on a Philip-X' Pert X-ray diffractometer with a Cu $\text{K}\alpha$ X-ray source ($\lambda = 0.15418 \text{ nm}$). Fourier-transform infrared (FTIR) spectroscopy measurements were performed on Bruker Fourier transform spectrometer model VECTOR22 using KBr pellets. Electrochemical experiments were conducted with a CHI660B workstation (Shanghai Chenhua, Shanghai) in a three-electrode system. All electrochemical experiments were performed in a cell containing 20.0 mL of phosphate buffer solution (PBS, $0.1 \text{ mol} \cdot \text{L}^{-1}$) at room temperature and using a coiled platinum wire as the auxiliary electrode, a saturated calomel electrode (SCE) as the reference electrode, and the AgCl@PANI modified glassy carbon electrode (GCE) as the working electrode.

2 Results and discussion

Chitosan with excellent biodegradability, biocompatibility, and nontoxicity is an *N*-deacetylated derivative polyelectrolyte of chitin and the second-most abundant natural polysaccharide after cellulose^[15-17]. In the molecular structure (Scheme 1) of chitosan, the hydroxyl and amino groups are regularly arranged at the equatorial positions in the $\beta(1,4)$ -linked *D*-glucosamine repeating units. It can act as a stabilizer to promote the interaction between inorganic materials and PANI.



Scheme 1 Chemical structure of chitosan

AgCl@PANI core-shell nanocomposites were synthesized through a facile one-step process in the presence of chitosan. The core-shell structure can be confirmed by TEM as shown in Fig.1. The dark spots inside the nanoparticles correspond to AgCl that is

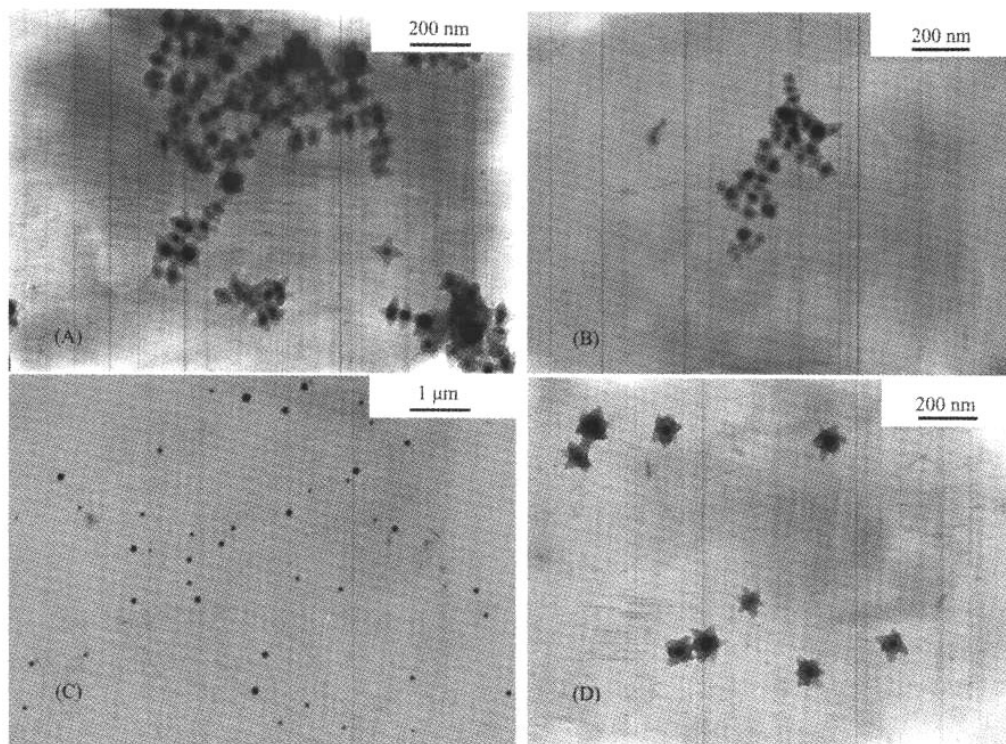


Fig.D is the TEM image with high magnification of (C)

Other synthesis conditions: AgNO_3 0.01 g; aniline 0.05 mmol; $n_{\text{Ag}}:n_{\text{AP}} = 1:1$; reaction time 24 h

Fig.1 TEM images of AgCl@PANI core-shell nanocomposites synthesized in different concentrations of chitosan: (A) 0.2%; (B) 0.5%; (C) and (D) 1%

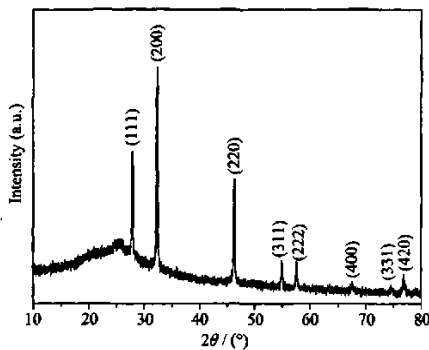
surrounded by a layer of PANI matrix. When the chitosan concentrations were 0.2% and 0.5%, the obtained AgCl@PANI nanocomposite with a diameter in the range of 40~120 nm was conglomerated. When the chitosan concentration increased from 0.5% to 1%, highly dispersed AgCl@PANI core-shell nanostructure with a shell thickness of 30~80 nm and a core diameter of 25~60 nm could be obtained. It should be noted that most of the as-prepared nanocomposites had a star-like structure. During the process for the formation of AgCl@PANI core-shell nanoparticles, after HCl aqueous solution of ammonium persulfate was added dropwise to chitosan solution containing AgNO_3 and aniline, a white AgCl precipitate appeared immediately and gradually turned blue. In the experiment, chitosan as an anchor agent plays an important role. Without chitosan, the core-shell structure could not be formed. Chitosan is a useful stabilizer that can promote a strong

interaction between AgCl particles and aniline monomer. For example, it has been used successfully in the preparation of uniform AgCl/polypyrrole core-shell particles^[8].

The XRD pattern confirms the presence of AgCl nanoparticles in the composites, as shown in Fig.2. The broad diffraction peak appeared at 2θ value of 25° is ascribed to the periodicity parallel to the polymer chains of PANI^[9]. Another eight diffraction peaks above 25° (2θ) correspond to Bragg deflections from (111), (200), (220), (311), (222), (400), (331), and (420) planes of AgCl. They are in good agreement with the reported data (PDF No.06-0480), showing the existence of AgCl nanoparticles in the AgCl@PANI core-shell composites.

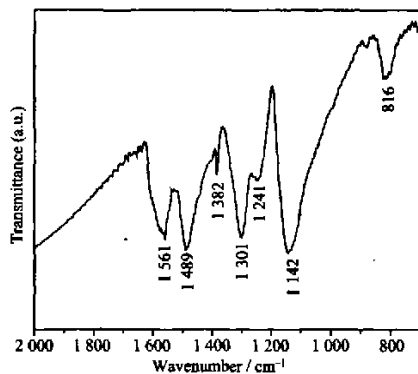
The FTIR spectrum of the AgCl@PANI is shown in Fig.3. The characteristic peaks at 1561 cm^{-1} and 1489 cm^{-1} correspond to the C=C stretching of quinoid and benzenoid rings^[20], 1301 cm^{-1} and 1241 cm^{-1} are

related to the C-N and C=N stretching modes^[21], 1 142 cm^{-1} is assigned to the in-plane bending of C-H^[22], and 816 cm^{-1} is attributed to the out-of-plane bending of C-H^[23]. Furthermore, an absorption band assignable to NO_3^- is observed at 1 382 cm^{-1} . This suggests that the obtained PANI in the composite was doped by NO_3^- .



Synthesis conditions: AgNO_3 0.01 g; aniline 0.05 mmol; $n_{\text{Ag}}/n_{\text{PANI}} = 1:1$; chitosan concentration 1%; reaction time 24 h

Fig.2 XRD pattern of AgCl@PANI core-shell nanocomposite

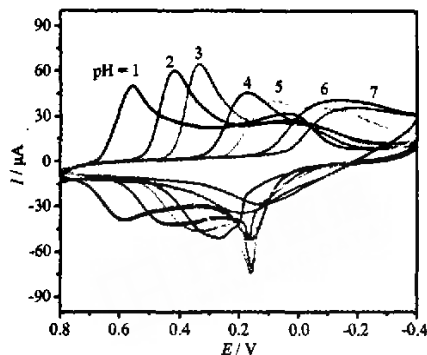


Synthesis conditions: AgNO_3 0.01 g; aniline 0.05 mmol; $n_{\text{Ag}}/n_{\text{PANI}} = 1:1$; chitosan concentration 1%; reaction time 24 h

Fig.3 FTIR spectrum of AgCl@PANI core-shell nanocomposite

The bare GCE was tested by cyclic voltammetric (CV) in different pH values of phosphate buffer solutions (PBS) before it was drop-coated by AgCl@PANI composite. It presents no redox process in the potential range studied. The working electrode coated with the composite was immersed in the electrolyte solution for 30 min prior to the measurement to assure diffusion of the solution into the interlayer space and permit a better ionic exchange. Fig.4 gives the cyclic voltammograms of AgCl@PANI modified GCE measured in different pH PBS at a scan rate of

100 $\text{mV} \cdot \text{s}^{-1}$.



Synthesis conditions: AgNO_3 0.01 g; aniline 0.05 mmol; $n_{\text{Ag}}/n_{\text{PANI}} = 1:1$; chitosan concentration 1%; reaction time 24 h

Fig.4 Cyclic voltammograms of AgCl@PANI core-shell nanocomposite modified GCE measured in different PBS pH buffers at a scan rate of 100 $\text{mV} \cdot \text{s}^{-1}$

PANI shows two separate redox peaks at pH value of 1 PBS. However, these two redox peaks move closer as the pH value of the solution is increased, and finally they merge to show only one broad redox peak when the pH value is 4. It is well known that PANI exists in three well-defined oxidation states: leucoemeraldine, emeraldine and pernigraniline. In the leucoemeraldine state all the nitrogen atoms are amines, but in pernigraniline the nitrogen atoms are imines. The amine/imine ratio in emeraldine is ~ 1 . Furthermore, emeraldine can be in its base or salt form, depending on the pH value. The first oxidation wave is assigned to the transition of leucoemeraldine to emeraldine salt and the second oxidation wave is due to the transition from emeraldine salt to pernigraniline state^[24]. The broad redox peak is observed at pH value of 4 in PBS for the sample with the redox potential around 0.2 V. This redox peak is the overlap of two redox processes normally found for the PANI system in acidic conditions^[25], as confirmed by the redox behavior of the composites measured in different PBS pH values. This electrochemical behavior of AgCl/PANI is also similar to that of PANI/carbon nanotube multilayer films prepared by the layer-by-layer method^[26].

In the CV curves, it is clear that the AgCl/PANI core-shell composites show good redox activity not only

at acidic solution but also at neutral pH environment in PBS. It is well known that silver halides are one type of important semiconductors. Although AgCl particles do not make a continuous electron path, the incorporated conducting AgCl provides more active sites for the charge transfer through the interface inside the electrode by making good contacts with the PANI matrix. Therefore, PANI particles located far from the electrode surface can effectively take part in the redox reaction. Meanwhile, we believe that more studies are needed to investigate the exact mechanism for the enhancement in electroactivity. The AgCl@PANI core-shell composites with good electrochemical activity have the potential application in the area of biosensor.

3 Conclusion

We have demonstrated the one-step synthesis of AgCl@PANI core-shell nanostructures in the presence of chitosan. Chitosan as a useful anchor agent promote a strong interaction between AgCl particles and aniline monomer leading to the formation of AgCl@PANI core-shell structure. The core-shell structure was characterized by TEM, XRD, FTIR and CV. In the CV measurements, it was found that the AgCl@PANI nanocomposites showed one well-defined pair of redox peaks in neutral pH environment.

References:

- [1] Huang J, Kaner R B. *J. Am. Chem. Soc.*, **2004**,**126**(3):851~855
- [2] Athawale A A, Bhagwat S V. *J. Appl. Polym. Sci.*, **2003**,**89**(9): 2412~2417
- [3] Gangopadhyay R, De A. *Chem. Mater.*, **2000**,**12**(3): 608~622
- [4] Huang J X, Virji S, Weiller B H, et al. *J. Am. Chem. Soc.*, **2003**,**125**(2):314~315
- [5] Liu H, Hu X B, Wang J Y, et al. *Macromolecules*, **2002**,**35**(25):9414~9419
- [6] Tian S J, Liu J Y, Zhu T, et al. *Chem. Mater.*, **2004**,**16**(21): 4103~4108
- [7] Riede A, Helmstedt M, Riede V, et al. *Langmuir*, **2000**,**16**(15): 6240~6244
- [8] Hao L Y, Zhu C L, Chen C N, et al. *Synth. Met.*, **2003**,**139**(2): 391~396
- [9] Chen A, Wang H, Li X. *Chem. Commun.*, **2005**:1863~1864
- [10] Lahav M, Weiss E A, Xu Q, et al. *Nanoletters*, **2006**,**6**(9): 2166~2171
- [11] Tian S J, Liu J Y, Zhu T, et al. *Chem. Mater.*, **2004**,**16**(21): 4103~4108
- [12] Bartlett P N, Simon E. *Phys. Chem. Chem. Phys.*, **2000**,**2**(11): 2599~2606
- [13] Bartlett P N, Wallace E N K. *J. Electroanal. Chem.*, **2000**,**486**(1):23~31
- [14] Raitman O A, Katz E, Buckmann A F, et al. *J. Am. Chem. Soc.*, **2002**,**124**(22):6487~6496
- [15] Yamamoto H, Amaike M. *Macromolecules*, **1997**,**30**(13):3936~3937
- [16] Bhattarai N, Edmondson D, Veisoh O, et al. *Biomaterials*, **2005**,**26**(31):6176~6184
- [17] Renbutsu E, Hirose M, Omura Y, et al. *Biomacromolecules*, **2005**,**6**(5):2385~2388
- [18] Cheng D, Xia H, Chan H. *Langmuir*, **2004**,**20**(23):9909~9912
- [19] Pillalamarri S K, Blum F D, Tokuhiko S T, et al. *Chem. Mater.*, **2005**,**17**(2):227~229
- [20] Huang K, Wan M X. *Chem. Mater.*, **2002**,**14**(8):3486~3492
- [21] McCarthy P A, Huang J, Yang S C, et al. *Langmuir*, **2002**,**18**(1):259~263
- [22] Li G C, Zhang Z K. *Macromolecules*, **2004**,**37**(8):2683~2685
- [23] Trakhtenberg S, Hangan-Balkir Y, Warner J C, et al. *J. Am. Chem. Soc.*, **2005**,**127**(25):9100~9104
- [24] Park M K, Onishi K, Locklin J, et al. *Langmuir*, **2003**,**19**(20): 8550~8554
- [25] Baba A, Tian S J, Stefani F C, et al. *J. Electroanal. Chem.*, **2004**,**562**(1):95~103
- [26] Liu J Y, Tian S J, Knoll W. *Langmuir*, **2005**,**21**(12):5596~5599

构

作者: 冯晓苗, 叶青青, 侯文华, 朱俊杰, [FENG Xiao-Miao](#), [YE Qing-Qing](#), [HOU Wen-Hua](#), [ZHU Jun-Jie](#)
作者单位: 南京大学化学化工学院, 南京, 210093
刊名: 无机化学学报 [|ISTIC|SCI|PKU](#)
英文刊名: [CHINESE JOURNAL OF INORGANIC CHEMISTRY](#)
年, 卷(期): 2007, 23(9)
被引用次数: 0次

参考文献(26条)

1. [Huang J. Kaner R B 查看详情](#) 2004(03)
2. [Athawale A A. Bhagwat S V 查看详情](#) 2003(09)
3. [Gangopadhyay R. De A 查看详情](#) 2000(03)
4. [Huang J X. Virji S. Weiller B H 查看详情](#) 2003(02)
5. [Liu H. Hu X B. Wang J Y 查看详情](#) 2002(25)
6. [Tian S J. Liu J Y. Zhu T 查看详情](#) 2004(21)
7. [Riede A. Helmstedt M. Riede V 查看详情](#) 2000(15)
8. [Hao L Y. Zhu C L. Chen C N 查看详情](#) 2003(02)
9. [Chen A. Wang H. Li X 查看详情](#) 2005
10. [Lahav M. Weiss E A. Xu Q 查看详情](#) 2006(09)
11. [Tian S J. Liu J Y. Zhu T 查看详情](#) 2004(21)
12. [Bartlett P N. Simon E 查看详情](#) 2000(11)
13. [Bartlett P N. Wallace E N K 查看详情](#) 2000(01)
14. [Raitman O A. Katz E. Buckmann A F 查看详情](#) 2002(22)
15. [Yamamoto H. Amaike M 查看详情](#) 1997(13)
16. [Bhattarai N. Edmondson D. Veiseh O 查看详情](#) 2005(31)
17. [Renbutsu E. Hirose M. Omura Y 查看详情](#) 2005(05)
18. [Cheng D. Xia H. Chan H 查看详情](#) 2004(23)
19. [Pillalamarri S K. Blum F D. Tokuhira S T 查看详情](#) 2005(02)
20. [Huang K. Wan M X 查看详情](#) 2002(08)
21. [McCarthy P A. Huang J. Yang S C 查看详情](#) 2002(01)
22. [Li G C. Zhang Z K 查看详情](#) 2004(08)
23. [Trakhtenberg S. Hangan-Balkir Y. Warner J C 查看详情](#) 2005(25)
24. [Park M K. Onishi K. Locklin J 查看详情](#) 2003(20)
25. [Baba A. Tian S J. Stefani F C 查看详情](#) 2004(01)
26. [Liu J Y. Tian S J. Knoll W 查看详情](#) 2005(12)

相似文献(5条)

1. 学位论文 隋晓萌 反胶束法合成聚苯胺-无机物复合纳米粒子 2003

该文采用三种不同的表面活性剂即阴离子型表面活性剂非离子型表面活性剂AOT(2-乙基己基琥珀酸钠)、Triton-X100或OP(聚氧乙烯烷基苯基醚)和阳离子型表面活性剂CTAB(十六烷基三甲基氯化铵)分别构建反胶束体系作为微反应器合成含有不同无机物内核(硫酸钡和氯化银)的聚苯胺-无机物复合纳

米粒子,并在OP、AOT体系和CTAB体系中分别合成了具有一定微观结构的聚苯胺-二氧化钛复合纳米粒子,初步探讨了在反胶束水池中合成具有微观结构的纳米粒子的机理。在AOT体系中合成聚苯胺-硫酸钡复合纳米粒子时,分别考察了搅拌因素和不同合成步骤对聚苯胺-硫酸钡尺寸及形态的影响,结果表明若想制备分布均匀,尺寸较小并且呈球形的复合纳米粒子应采用一步合成并在反应进行过程中伴随搅拌。利用透射电子显微镜(TEM)、扫描电子显微镜(SEM)、红外光谱(IR)、紫外-可见光谱(UV-vis)、热失重分析(TGA)、X-射线衍射(XRD)和四探针电导率仪等测试手段对产物的形态、结构、结晶性、热稳定性和导电性等性质进行了一系列的表征。

2. 学位论文 杨晓明 微米/纳米结构导电高分子 2006

自从导电聚合物在二十世纪七十年代末期被人们发现以来,既具有导电性又具有高分子性质的导电聚合物材料引起了人们的广泛关注,并已成为科学研究的另一大热点。由于导电聚合物具有密度小、质量轻、导电性能可以根据使用需要在导体、半导体和绝缘体之间进行调节等一系列优点,目前已经在金属防腐、高能电池、微波吸收等领域得到初步的应用。

近年来,低维材料,尤其是纳米材料的发展给物理、化学、材料、生物、信息等基础与应用领域带来了新的机会与活力。这一技术必将带来新的功能材料和具有卓越性能的功能器件,对人类未来生活产生深远的影响。材料的微米/纳米结构化有利于材料的集成与组装,同时能为材料带来相应的尺寸效应和空间效应,提高材料的性质,丰富材料的功能。导电高分子纳米材料通常分为纳米管(线),纳米复合材料及其空心结构以及其它一些具有特殊形貌的具有纳米/微米结构的导电高分子。目前人们对高分子材料的分子结构、制备过程对微米/纳米结构材料性能的影响还不十分清楚。每一种制备技术通常只适用于一些特殊的导电高分子,且效率较低,从而限制了材料的广泛应用。因此,进一步探索材料的生长与组装机理,进一步开发普通、高效的导电高分子微米/纳米结构的加工技术既具有重要的理论意义,也有明显的实用价值。

本文在开发新的导电高分子合成手段来制备高性能的导电高分子微米/纳米结构材料;研究导电高分子微米/纳米结构材料的控制生长技术;表征和测试材料的结构、形貌和性能等方面进行了探索,并得到了一些新的结果。

(1) 导电高分子纳米管的制备

本文提出了一种既具有“无模板法”简便易行的优点又具有“硬模板法”普适性的新体系来制备导电高分子纳米管(线)。同时作为掺杂剂和模板剂的甲基橙分子与氧化剂三氯化铁形成纤维状的可反应性沉淀。吡咯单体在这种纤维状沉淀表面氧化聚合,同时由于三价铁离子被还原而使沉淀发生自降解,最终得到了即具有光电转换功能又具有导电性的聚吡咯纳米管。这种聚吡咯纳米管由甲基橙、氯离子以及微量的铁离子复合物(FeCl₄⁻)掺杂,掺杂率为0.36,并具有较高的分子链规整性,电导率为96S/cm。惰性气氛下煅烧可得到碳纳米管,这为碳纳米管的制备提供了一种新的途径。

(2) 无机材料—导电高分子纳米微米复合物的制备

与常规高分子不同,导电高分子由于其不溶不熔的性质使其非常难以加工。因此,人们在发展新的方法来改善导电高分子的加工性方面作了很多努力。其中引起人们广泛兴趣的一种方法为在无机或者有机纳米颗粒表面均匀沉积一层导电高分子层,制备具有胶体稳定性的复合材料。本文首次将壳聚糖吸附在二氧化硅表面,然后通过自组装的方法成功的制备了“向日葵”型二氧化硅/聚吡咯复合纳米颗粒,即130nm左右的聚吡咯小球均匀生长在500nm的二氧化硅表面,壳聚糖分子链存在于聚吡咯小球的间隙中。这种特殊的结构使得这种复合颗粒既具有高的电导率,同时又具有一定的胶体稳定性。此外,本文采用二氧化硅表面预硫化处理,在高分子稳定剂PVP存在下聚合吡咯单体,成功的得到了分散性良好的导电聚吡咯—二氧化硅复合微球。

(3) 金属—导电高分子纳米微米复合物的制备

在金属纳米颗粒表面修饰导电高分子如聚吡咯或聚苯胺已经成为纳米复合材料中很有意义的一部分。在制备金属胶体的过程中如果还原剂是一种单体且能够氧化聚合,那么将很方便的得到导电高分子与金属的复合材料。在本文中,我们用UV来诱导硝酸银氧化聚合吡咯单体,单体的聚合与金属的还原同时进行,在稳定剂PVP存在下,一步即可生成具有核/壳结构的银/聚吡咯纳米颗粒,而不是生成金属颗粒与聚吡咯的混合物。

(4) 共离子法制备导电高分子空心球

本文报道了一种共离子法一步完成氯化银为核聚吡咯为壳的纳米复合材料的制备。在合成该核/壳结构纳米粒子的过程中,采用三氯化铁作为吡咯聚合的氧化剂,壳聚糖作为稳定剂,硝酸银提供银离子的来源。三氯化铁滴加入含有吡咯单体、硝酸银、壳聚糖的均一混合溶液中时,氯离子与银离子结合生成白色的氯化银沉淀,同时三价铁离子氧化吡咯单体,并在吸附了壳聚糖的氯化银颗粒表面成核聚合,最终一步得到了氯化银/聚吡咯核壳结构的纳米粒子。进一步将作为模板的氯化银颗粒溶解,可得到聚吡咯的纳米空心球。此空心球的壳厚可由加入的吡咯单体的量控制。(5) LbL自组装法制备导电高分子空心球

纳米/微米级中空功能小球由于其广阔的应用前景引起人们的广泛兴趣,但通常的牺牲模板的方法制备空心球往往会破坏空心球的结构。本文在带负电荷的聚苯乙烯胶体颗粒表面先层层自组装带阳离子的壳聚糖以及带阴离子的聚苯乙烯磺酸钠,然后用戊二醛交联壳聚糖层以提高聚电解质多层膜的强度,最后将聚苯乙烯溶解得到自支撑的具有较好的电导率及良好的物理化学稳定性使其在DNA电化学传感器领域有着良好的应用前景。这种方法制备的中空聚吡咯小球的结构不会由于核的溶解受到破坏,同时得到的聚吡咯壳层较疏松,可望在生物和医药领域得到广泛应用。

3. 学位论文 袁莹 一维导电聚苯胺纳米阵列在DNA电化学传感器中的应用 2008

前言:

DNA生物传感器是以DNA作为敏感单元,对与其互补的靶DNA进行检测的方法—即利用单链DNA(ssDNA)之间的互补杂交关系进行检测。DNA电化学传感器具有检测速度快、方法简便、仪器性价比高等特点,因而最有希望成为大规模商业应用的传感器。但是这些传感器还存在选择性不好、灵敏度不高,稳定性不强等缺点。把纳米技术与核酸检测技术融为一体制备成新型的纳米生物传感器是解决电化学传感器的缺点的一种有效的办法。

导电聚苯胺纳米材料具有较高的电导率及良好的物理化学稳定性使其在DNA电化学传感器领域有着良好的应用前景。本文利用模板法和电化学自组装法将一维导电聚苯胺纳米阵列合成在石墨电极的表面。由于聚苯胺纳米阵列修饰的石墨电极提供了较大的有效表面积,使其固化的单链DNA探针的数量得到了数量级的增加,同时由于聚苯胺纳米阵列的排列的高度有序性,为DNA的杂交提供了优良的动力学条件和微环境,因此DNA杂交的检测灵敏度得到大幅的提高。

本文利用这两种方法制备了DNA电化学传感器,并对其检测特性进行了表征和评估。在优化了实验条件(杂交温度、杂交时间、指示剂)后,考察了DNA电化学传感器的检测灵敏度。检测结果显示利用一维导电聚苯胺纳米阵列制备的DNA电化学传感器的检测灵敏度可以达到1fmol/L,并在靶标寡核苷酸的不同浓度范围内具有良好的线性响应。

实验材料与方法:

1、实验材料

本实验所需的寡核苷酸均购买自大连宝生物技术公司。本实验采用的试剂其纯度皆为分析纯以上级,没有进一步纯化。配置溶液的实验用水为超纯水机过滤的超纯水。本实验所用的石墨电极为自制电极,饱和银-氯化银电极、铂片电极、铂丝电极均购买自上海精密科学仪器有限公司。

2、一维导电聚苯胺纳米阵列修饰的DNA电化学传感器的制备

本实验分别采用了氧化钨模板法和电化学自组装法在预处理过的石墨电极上合成一维导电聚苯胺纳米阵列,并在聚苯胺纳米纤维上共价固定了寡核苷酸探针,以此构成了DNA电化学传感器。

3、DNA电化学传感器的电化学测试

首先,本实验对电化学传感器检测时的杂交条件(杂交温度和杂交时间)进行了系统的筛选。

然后,本实验考察了两种电化学杂交指示剂(道诺霉素和茂铁)对检测灵敏度的影响。在研究中,利用循环伏安法和差分脉冲伏安法扫描来确定其峰电位。

最后,对两种方法制备的DNA电化学传感器分别进行重复性和稳定性的检测。

实验结果:

1、一维导电聚苯胺纳米阵列修饰的DNA电化学传感器的制备

显微形态学和电化学表征的结果显示利用两种制备方法可以将一维导电聚苯胺纳米阵列很好地整合在石墨电极的表面。荧光显微镜检测的结果也证实了寡核苷酸探针在聚苯胺纳米纤维上的固定。

2、杂交反应

实验结果显示杂交温度为53.7℃和杂交时间为1小时的杂交条件是该传感器的最适工作条件。

3、DNA电化学传感器的电化学测试

对于模板法制备的DNA电化学传感器,道诺霉素的峰电流与靶标寡核苷酸在7.557~755.7fmol/L的浓度范围内显现了良好的线性关系(R²=0.9817),并给出了1fmol/L的检测下限;对于电化学自组装法制备的DNA的电化学传感器,道诺霉素的峰电流与靶标寡核苷酸在

0.7557~6.0456nmol/L的浓度范围内具有良好的线性关系($R^2=0.9858$),并得到了75.5pmol/L的检测下限。而在利用二茂铁作为指示剂的检测中,二茂铁的还原峰电流与靶标寡核苷酸的浓度在15.83nmol/L到126.64nmol/L范围内表现了良好的线性关系($R^2=0.9835$)。

4、重复性测试实验结果显示

利用两种方法制备的电化学传感器在三次连续重复测量中显示了良好的稳定性。

讨论和结论:

本实验利用两种不同方法制备了一维导电聚苯胺纳米阵列结构—模板法和电化学自组合法。形态学表征中两种阵列都显示了良好的均一性和定向排列特性,电化学表征也表明一维聚苯胺纳米阵列修饰的石墨电极具有比裸石墨电极和聚苯胺膜修饰的石墨电极大得多的比表面积。这些都为我们进一步利用这种阵列修饰石墨电极以及制备高灵敏度的DNA电化学传感器提供了良好的基础。由于聚苯胺纳米阵列修饰的石墨电极提供了较大的有效表面积,使聚苯胺纳米阵列中的每根聚苯胺纳米线如同一个收集杂交信号的纳米器件,同时由于聚苯胺纳米阵列的排列的高度有序性,为DNA的杂交提供了优良的力学条件和微环境,因此DNA杂交的检测灵敏度得到大幅度的提高。这为进一步利用这种阵列修饰石墨电极而制备DNA电化学传感器提供了良好的可行条件。

实验结果表明电化学自组合法制备的DNA电化学传感器的灵敏度低于模板法制备的DNA电化学传感器。认为这可能是由于利用不同方法制备的聚苯胺纳米阵列的形态差异而导致的。

还观察到DNA电化学传感器的灵敏度直接依赖于杂交指示剂对双链DNA的选择性。检测结果显示无论是道诺霉素还是二茂铁,其峰电流在靶标寡核苷酸的不同的浓度范围内均取得了良好的线性响应,但二茂铁作为杂交指示剂的灵敏度低于道诺霉素,主要的原因是作为杂交指示剂它们与DNA的结合方式不同。

4. 期刊论文 隋晓萌,褚莹,邢双喜,吴子生 反胶束体系中合成聚苯胺-无机物复合纳米微粒 -化学学报2004, 62(1)

利用阴离子型表面活性剂2-乙基己基琥珀酸钠(AOT)形成的反胶束作为微反应器合成了聚苯胺-氯化银和聚苯胺-硫酸钡复合纳米粒子;考察了搅拌因素和不同合成步骤对聚苯胺-硫酸钡尺寸及形态的影响;并利用TEM, IR, UV-vis, XRD和四探针电导率仪对产物进行了表征。研究结果表明,反胶束法可以有效地应用于有机-无机复合纳米材料的制备。

5. 学位论文 莫尊理 反胶束模板-原位聚合纳米复合技术及三元复合材料的研究 2006

聚合物/石墨纳米复合材料具有一些独特的物理、力学性能,是目前材料科学研究领域的前沿课题,近年来,国际上对聚合物/层状硅酸盐纳米复合材料进行了大量的研究,提出了一些插层复合理论,但对弱极性、非极性聚合物的插层复合及聚合物/无机纳米粒子/层状无机物三元或多元纳米复合材料的制备及其性能的研究才刚刚起步,本论文借助反胶束“微反应器”和原位聚合纳米复合技术实现层状无机物的层间剥离和与聚合物的纳米复合,是对现有纳米复合技术和纳米复合材料的发展和完善,建立了反胶束模板。原位聚合纳米复合新技术,实现了膨胀石墨的层间滑移、片层剥离,及膨胀石墨(EG)或纳米石墨微片(NanoG)与聚甲基丙烯酸甲酯(PMMA)或聚苯胺(PANI)和无机纳米粒子的纳米复合,成功制备了PMMA/Eu(OH) \langle 3 \rangle /EG、PMMA/Ni(OH) \langle 2 \rangle /EG、PMMA/Ce(OH) \langle 3 \rangle -Pr \langle 2 \rangle O \langle 3 \rangle /NanoG、PANI/Ce(OH) \langle 3 \rangle -Pr \langle 2 \rangle O \langle 3 \rangle /NanoG、PPy/AgCl/NanoG三元纳米复合材料;对该新型纳米复合材料做了详细的表征与分析;系统研究了三元纳米复合体系的复合过程和机理,论述了PANI/Ce(OH) \langle 3 \rangle -Pr \langle 2 \rangle O \langle 3 \rangle /NanoG纳米复合材料的导电性能及导电机理;研究了这些纳米复合材料的热稳定性及其影响因素,探究纳米复合材料的导电、热稳定性理论;获得了兼具优良导电和热稳定性的三元纳米复合材料。同时进一步拓展了反胶束“微反应器”的应用领域。同时对NanoG/AgCl/PPy进行了跨尺度的分子动力学和平均场密度泛函模拟研究。

建立了反胶束模板、原位聚合纳米复合新技术,选用MMA或苯胺,稀土离子(Eu \langle 3 \rangle , Pr \langle 3 \rangle , Ce \langle 3 \rangle)或过渡金属离子(Ni \langle 2 \rangle)与EG或NanoG为对象,利用反胶束模板-原位聚合复合技术,制备PMMAfEu(OH) \langle 3 \rangle /EG、PMMA/Ni(OH) \langle 2 \rangle /EG、PMMA/Ce(OH) \langle 3 \rangle -Pr \langle 2 \rangle O \langle 3 \rangle /NanoG和PANI/Ce(OH) \langle 3 \rangle -Pr \langle 2 \rangle O \langle 3 \rangle /NanoG、三元纳米复合材料。

反胶束模板为有机单体和无机粒子向膨胀石墨的片层之间扩散,形成纳米复合结构创造了条件。一方面,反胶束模板中的表面活性剂既组装形成了反胶束“微反应器”以制备粒径分布均匀的无机纳米粒子,又作为石墨和无机纳米粒子的表面修饰剂,以提高其与聚合物单体的相容性及亲和力。另一方面,由于反胶束“微反应器”尺寸小且分布均匀限制了纳米粒子的生长空间,使得无机相与有机相在反应过程中分散均匀,有效地解决了纳米粒子的团聚问题,并达到纳米尺度的均匀分散。而石墨具有弱的层间结构,是实现层间剥离和纳米复合的结构基础。

反胶束模板-插层原位聚合纳米复合技术实现石墨的层间剥离及与PMMA和无机纳米粒子的纳米复合是分阶段完成的。通过控制条件可分别制备插层型和剥离型纳米复合材料。插层型纳米复合有利于形成导电网络,是制备导电复合材料所追求的结构。剥离型复合可同步实现增强、增韧,提高材料的力学性能。深入研究了聚合物/无机纳米粒子/石墨三元纳米复合材料结构及其相关性,借助现代分析检测技术,研究了聚合物/无机纳米粒子/石墨三元纳米复合材料的结构,石墨在不同基体的分散程度,石墨、无机纳米粒子的加入对复合材料热稳定性性能的影响等。通过该方法解决纳米石墨的易团聚、不易工业化的缺点。

利用反胶束模板、原位聚合纳米复合技术制备的三元纳米复合材料中石墨粒子具有大的尺寸、形状比和占有体积。无机纳米粒子在纳米复合材料中分布均匀,且可发生自组装形成棒状或树枝状结构,这种微结构有利于增强无机纳米粒子与纳米石墨微片及聚合物基体之间的界面亲和力,致使该复合材料的热稳定性明显提高。

探索了PANI/Ce(OH) \langle 3 \rangle -Pr \langle 2 \rangle O \langle 3 \rangle /NanoG纳米复合体系纳米复合体系的导电逾渗规律,实现了低填充、高电导率复合材料制备的技术途径,揭示了该体系的导电机理。PANI/Pr \langle 2 \rangle O \langle 3 \rangle -Ce(OH) \langle 3 \rangle /NanoG三元纳米复合材料具有纳米分散复合结构,通过石墨纳米片层的相互搭接形成导电网络,同时与聚苯胺形成具有纳米间隙的石墨网络,构成点、键和曲面复合配位模式的导电多面体,使石墨粒子的有效半径大大延伸,导电电荷不再局域于某一粒子,而在导电多面体间跃迁,容易形成隧道电流,所以具有极低的导电逾渗阈值,低于1.0 wt%。

结合微乳液聚合和原位聚合两种技术,制备出纳米聚吡咯/氯化银/石墨(PPy/AgCl/NanoG)复合材料,利用原位聚合方法制备了NanoG/AgCl/PPy复合材料。并进行了跨尺度的分子动力学和平均场密度泛函模拟研究。结果表明,体系结构为聚吡咯平行包覆在石墨上,AgCl存在于聚吡咯的空腔中,从而形成了稳定的三元纳米复合材料。材料电导率的测试结果表明,引入导电性优良的纳米石墨薄片,为聚吡咯的网络结构提供导电通路,宏观表现为材料的电导率明显增加。差热-热重分析说明NanoG/AgCl/PPy复合材料的环境稳定性要明显优于纯聚吡咯。在介观尺寸上,复合体系中三种物质大部分复合均匀,在纳米水平上存在大量的界面,势能较高;但有少量的聚集,其中以AgCl最易发生聚集。体系中三种物质不易发生相分离。

本论文研究结果表明,反胶束模板-原位聚合纳米复合技术是制备兼具优良导电、耐热的三元石墨纳米复合材料的新方法,同时对类似石墨的层状化合物如蒙脱土复合纳米材料的制备也比较适用,是实现高分子复合材料的功能化和高性能化的有效途径,丰富和发展了纳米复合技术,拓展了高分子材料的应用领域。

本文链接: http://d.wanfangdata.com.cn/Periodical_wjhxsb200709013.aspx

授权使用: 赵华(wfnjdx), 授权号: 06258e78-d510-499d-b4a6-9df600e79553

下载时间: 2010年9月19日